# PROFILED POLYETHYLENE TEREPHTHALATE FILAMENTS THAT INCORPORATE COLLAGEN AND CALCIUM PHOSPHATE ENHANCE LIGAMENTISATION AND BONE FORMATION

C.C. Tai[1,§], C.C. Huang[2,§], B.H. Chou[3], C.Y. Chen[4], S.Y. Chen[2], Y.H. Huang[1,5,6], J.S. Sun[7] and Y-H. Chao[3,*]

[1] International Ph.D program for Cell Therapy and Regeneration Medicine, College of Medicine, Taipei Medical University, Taipei, Taiwan
[2] Department of Materials Science and Engineering, National Yang Ming Chiao Tung University, Hsinchu, Taiwan
[3] School and Graduate Institute of Physical Therapy, College of Medicine, National Taiwan University, Taipei, Taiwan
[4] Department of Orthopaedics, Shuang Ho Hospital, Taipei Medical University, New Taipei City, Taiwan
[5] Department of Biochemistry and Molecular Cell Biology, School of Medicine, College of Medicine, Taipei Medical University, Taipei, Taiwan
[6] TMU Research Centre of Cell Therapy and Regeneration Medicine, Taipei Medical University, Taipei, Taiwan
[7] Department of Orthopaedics, School of Medicine, China Medical University, Tai-Chung, Taiwan
[§] There authors contributed equally to this work

**Abstract**

Polyethylene terephthalate (PET) artificial ligaments offer an unlimited source of ligaments without donor-site-related morbidity and with good mechanical properties for a rapid return to sporting activities. Developing PET artificial ligaments with excellent ligamentisation and ligament-bone healing is still a considerable challenge. This study aimed to investigate the effects of the profiled PET/collagen/calcium phosphate (PET/C/CaP) ligament upon cell growth, ligamentisation and ligament-bone healing *in vitro* and *in vivo*. Profiled PET/C/CaP filaments were made by melt-spinning process with 2 % CaP hybrid spinning and collagen coating. Rat mesenchymal stem cells (MSCs) were cultured on the profiled PET/C filaments for cytotoxicity, viability, scanning electron microscopy (SEM) and ligament-related gene expression analysis. MSCs' osteogenic capacity on the profiled PET/CaP filaments was identified by detecting osteogenic gene expression and alizarin red S staining. For *in vivo* verification, an animal study was performed to evaluate the effect of the profiled PET/C/CaP ligament in a rabbit knee medial collateral ligament reinforcement reconstruction model. The graft ligamentisation and bone formation were investigated by SEM, histology, microcomputed tomography and mechanical tests. The profiled PET/C filaments enhanced MSC proliferation and ligament-related gene expression. Furthermore, they enhanced osteogenic gene expression, alkaline phosphatase activity and mineralisation of MSCs. The *in vivo* study indicated that the profiled PET/C/CaP ligament enhanced ligamentous matrix remodelling and bone formation. Therefore, their use is an effective strategy for promoting MSCs' ligamentous and osteogenic potential *in vitro* and enhancing ligamentous matrix remodelling and bone formation *in vivo*.

**Keywords**: Artificial ligament, polyethylene terephthalate, profiled filaments, calcium phosphate, ligamentisation, bone formation.

***Address for correspondence**: Dr Yuan-Hung Chao, School and Graduate Institute of Physical Therapy, College of Medicine, National Taiwan University No. 17, Xuzhou Road, Zhongzheng District, Taipei 10055, Taiwan.
Telephone number: +886 233668129 Email: yuanhungchao@ntu.edu.tw



**List of Abbreviations**

| | | | |
|---|---|---|---|
| | | ACL | anterior cruciate ligament |
| | | ALP | alkaline phosphatase |
| 2D | two dimensional | ANOVA | analysis of variance |
| 3D | three dimensional | BMP-2 | bone morphogenetic protein 2 |

| | |
|---|---|
| BMSC | bone marrow stromal cell |
| CaP | calcium phosphate |
| Col1a1 | collagen type I $\alpha$1 |
| Col3a1 | collagen type III $\alpha$1 |
| DAPI | 4′,6-diamidino-2-phenylindole |
| DMEM | Dulbecco's modified Eagle's medium |
| Egr1 | early growth response factor 1 |
| ELISA | enzyme-linked immunosorbent assay |
| eNOS | endothelial nitric oxide synthase |
| FOY | fully oriented yarn |
| GAPDH | glyceraldehyde-3-phosphate dehydrogenase |
| GPU | graphics processing unit |
| HA | hydroxyapatite |
| H&E | haematoxylin and eosin |
| LARS | Ligament Advanced Reinforcement System |
| LDH | lactic dehydrogenase |
| MCL | medial collateral ligament |
| MSC | mesenchymal stem cell |
| OCN | osteocalcin |
| OP | osteopontin |
| PBS | phosphate-buffered saline |
| PCL | polycaprolactone |
| PEG | polyethylene glycol |
| PET | polyethylene terephthalate |
| PET/C/CaP | polyethylene terephthalate/collagen/calcium phosphate |
| POY | pre-oriented yarn |
| RT-qPCR | quantitative reverse transcription polymerase chain reaction |
| Runx2 | runt-related transcription factor 2 |
| Scx | scleraxis |
| SD | standard deviation |
| SEM | scanning electron microscopy |
| Tnc | tenascin C |
| Tnmd | tenomodulin |
| VEGF | vascular endothelial growth factor |
| μCT | micro-computed tomography |

## Introduction

Ligament injuries are the most common pathology of the knee among athletes and ACL and MCL injuries account for most ligament problems (Bollen, 2000; Majewski *et al.*, 2006). Following a ligament injury, other complications, including joint instability, dislocation and osteoarthritis, can occur, causing functional disability and a great societal economic burden. Autologous grafts are commonly used for knee-ligament reconstruction. Autografts do not induce graft rejection; moreover, their natural properties and availability make them a first-line option. However, this process would cause donor-site pain, disability, crepitus, weakness of the extensor mechanism and patellar fracture following surgery (Bashaireh *et al.*, 2020; Höher *et al.*, 2003; Wood *et al.*, 2019). Although allografts may prevent donor-site problems, they may also induce disease transmission. The graft sterilisation process changes the properties of the ligament and elevates the associated costs (Höher *et al.*, 2003). To overcome the drawbacks of autografts and allografts, synthetic grafts are one of the most considered options for ligament reconstruction. The benefits of these grafts include no morbidity to the donor site and availability. Moreover, they provide the graft with strong mechanical properties and significantly diminish the time required to return to activity and training (Zoltan *et al.*, 1988). However, long-term follow-up showed a 33 % failure rate of synthetic grafts and several complications, such as synovitis, joint instability as well as problems with biocompatibility and durability (Satora *et al.*, 2017; Tulloch *et al.*, 2019a; Tulloch *et al.*, 2019b). Apart from the abovementioned scenarios, because synthetic grafts pass through bone tunnels and are fixed using screws, the synthetic material is not ideal for osseointegration.

PET artificial ligaments, such as the LARS® system (Surgical Implants and Devices, Arc-sur-Tille, France) are commonly used. However, well-visualised autologous tissue ingrowth is barely observed due to the hydrophobic nature of PET, which may lead to inferior biomechanical properties following reconstruction (Tulloch *et al.*, 2019c). To overcome these drawbacks, previous studies have focused on the modification of PET surface properties, including silk fibroin, HA and CaP (Cai *et al.*, 2018; Chen *et al.*, 2016; Zhi *et al.*, 2019). Current commercial products are made of cylindrical PET filaments (Yu *et al.*, 2014). The textile industry makes profiled cross-section filaments, such as + or Y shape, to produce moisture-wicking yarn. Polymer filaments with a profiled cross-section design help fluid to circulate through the gaps formed between the fibres by capillary action. The application of such profiled PET filaments to the artificial ligament design may help with cell growth and ligament maturation but the effect remains to be further verified.

Collagen plays an important role in the extracellular matrix: it has excellent biocompatibility, shows differential ligamentous induction and regulates fibroblast behaviour (Dong and Lv, 2016). Scaffold coating with type I collagen leads to a greater fibroblast infiltration depth and a higher infiltration ratio, suggesting that collagen may stimulate fibroblast migration and cell remodelling (Chang *et al.*, 2020). Cells isolated from the ACL and cultured on scaffolds comprised of type I collagen showed higher expression of the ligamentous gene *TNMD* and lower expression of the osteogenic differential gene *ALP* than elastin-A-manufactured scaffolds (Mizutani *et al.*, 2014). To facilitate ligamentisation of the synthetic graft, the collagen coated on PET filaments was adapted to create an environment suitable for ligament tissue regeneration and maturation.

CaP-based materials have been used in a variety of biomedical applications due to the benefits of good osteoconductive capacity, biocompatibility, bioactive properties and osseointegration (Meng *et al.*, 2016;

Overmann and Forsberg, 2020). *In vitro* culture of MC3T3-E1 mouse osteoblastic cells on PET artificial ligament with biomimetic nanoscale CaP coating demonstrated good biocompatibility for cell adhesion and proliferation and high ALP activity (Chen *et al.*, 2016). A recent study electrodepositing CaP onto PET artificial ligaments significantly improved the graft-bone integration process following ACL reconstruction (Cai *et al.*, 2021). A previous study showed that PET coated with HA, a type of CaP, could induce bone formation between grafts and natural bone, improving the mechanical properties (Li *et al.*, 2011). Dental implants coated with HA and collagen showed more bone formation and bone-to-implant contact than those coated with HA only (Lee *et al.*, 2014). Although several studies have reported using CaP on PET surface modification to enhance osteogenic activity, it remains a big challenge for artificial ligament reconstruction with distinct osseointegration of the ligament-bone insertion site.

The present study aimed to develop a new type of PET artificial ligament with profiled cross section filaments and biological modification. MSCs were cultured on the surface of profiled PET filaments incorporating collagen and CaP (profiled PET/C/CaP ligament) to assess the biocompatibility for cell proliferation and the induction of ligamentous and osteogenic potential *in vitro*. Moreover, an animal study was performed to evaluate the effect of profiled PET/C/CaP ligament in a rabbit knee MCL reinforcement reconstruction model. It is hypothesised that profiled PET/C/CaP ligament is an effective strategy for promoting MSC ligamentous and osteogenic potential *in vitro* and enhancing ligamentous matrix remodelling and bone formation *in vivo*.

## Materials and Methods

### MSC isolation and culture

Rat bone marrow MSCs were isolated from 12 8-week-old Sprague-Dawley rats. After the rats were euthanised, the bilateral tibiae and femora were detached and preserved in PBS. Tibia and femur bone marrows were flushed several times with DMEM containing 10 % FBS (Gibco) using a 5 mL syringe and then filtered through a 70 μm cell strainer. A total of 10 mL of bone marrow solution was centrifuged at 378 ×*g* for 5 min. The supernatant was discarded and the remaining marrow was resuspended in DMEM containing 10 % FBS. Then, cells were cultured in a 100 mm dish and incubated at 37 °C and 5 % humidified $CO_2$. To isolate the adherent cells, the culture medium was changed every 24 h, 3 times to complete the primary culture (passage 0). The culture medium was changed every 3 d and the cells were trypsinised and sub-cultured in 100 mm dishes after they reached 80 % confluence. Cells from passages 1 to 3 were used. The study procedures received approval from the Institutional Animal Care and Use Committee of National Taiwan University College of Medicine and College of Public Health (IACUC approval number 20180401) and the Guide for the Care and Use of Laboratory Animals (Chinese-Taipei Society of Laboratory Animal Science).

### Preparation and characterisation of the PET filaments

Profiled PET filaments were made by a melt-spinning process from the Industrial Technology Research Institute and Taiwan Textile Research Institute. The PET raw material particles were made into 4 Denier (D) pre-oriented yarn at a spinning temperature of 288 °C and a spinning speed of 2,500 m/min and then extended to 1.9 D fully oriented yarn at a temperature of 140 °C. The filament cross sections were varied by changing the spinneret hole shape. The profiled filaments included four shapes: O, I, Y and cross (+). Cross-section images were acquired using a Leica MZ12 Stereo microscope. In addition, the CaP bioceramic was predispersed, mixed with PET at 2 % (w/w) and, then, the melt-spinning method was used to make the PET/CaP filaments. Next, textile samples were assembled, with PET filaments as the longitudinal core and PET/CaP filaments woven at the two ends. Before collagen coating, the filaments were sterilised and dehydrated with alcohol. Following drying, the filaments were soaked in 1 % HCl solution for 2 h and washed in $ddH_2O$. The filaments were soaked in collagen solution several times and then put into a drying oven to complete the collagen coating (PET/C). Finally, the textile samples were rolled into a cylindrical shape as an artificial ligament for this experiment (Fig. 1).

### Cytotoxicity

An LDH Cytotoxicity Assay Kit-WST (Dojindo Molecular Technologies, Rockville, MD, USA) was used to test PET cytotoxicity. MSCs were seeded in 96-well plates and incubated for 24 h. Next, PET fibres were cut into pieces and added to the plates. Then, the LDH test protocol followed the guidelines of the kit.

### Cell viability

The Alamar Blue™ Cell Viability Reagent (Thermo Fisher) was used to test the cell viability. MSCs were seeded on profiled filament PET artificial ligaments at $6 \times 10^5$ cells/cm$^2$. At 7, 14 and 21 d, the culture medium was replaced with a medium containing 10 % alamar blue followed by incubation for 4 h. The absorption at 570 nm/600 nm was detected using an ELISA reader (Molecular Devices, San Jose, CA, USA).

### SEM

MSCs were seeded on profiled filament PET artificial ligaments for 7 d. SEM was used to observe cell proliferation. PET artificial ligaments were fixed using 2.5 % (v/v) glutaraldehyde in PBS at 4 °C for 24 h. After washing with PBS 3 times, the cells were immersed in 1 % (v/v) buffered osmium tetroxide (pH 7.4) for 1 h. Then, the samples were dehydrated

through a graded ethanol series (50 %, 75 %, 90 % and 95 %) for 10 min and then washed 3 times with 100 % ethanol for 10 min. The samples were dried using a critical point dryer, sputter-coated with gold (10 nm thick) and observed by SEM (JSM-5410, JEOL, Tokyo, Japan).

**Fluorescence microscope**

A LIVE/DEAD™ Viability/Cytotoxicity Kit (Thermo Fisher) was used to detect MSC proliferation on the profiled filament PET artificial ligaments. Following 14 d of incubation, the samples were washed with PBS 3 times. Then, 10 mL of PBS containing ethdium homodimer-1 and calcein AM working solution were added to the samples for 30 min, followed by washing with PBS. Before fluorescence microscopy (Zeiss AXIOVERT 200 M; excitation/emission: calcein AM 494/517 nm, ethdium homodimer-1 528/617 nm) was performed, 100 µL aqueous anti-fade mounting medium containing DAPI (ab104139, Abcam) was added at room temperature for 5 min.

**RNA extraction and RT-qPCR**

TRI Reagent® and a Direct-zol™ RNA Kit (Zymo Research, Irvine, CA, USA) were used to isolate total RNA. Total RNA was reverse-transcribed into cDNA using the PrimeScript™ RT reagent Kit (Takara, Kyoto, Japan). RT-qPCR was performed using the CFX Connect Real-Time PCR Detection System (Bio-Rad) with an iQ SYBR® SuperMix Kit (Bio-Rad), where each reaction mixture contained 50 ng of cDNA. The $2^{-\Delta\Delta Ct}$ method was used to calculate the gene expression level using *GAPDH* as an internal control. Primer sequences are listed in Table 1.

**Application of *in vitro* mechanical stretching**

*In vitro* uniaxial stretching was applied to the artificial ligaments to mimic the *in vivo* mechanical environment. To detect the influence of mechanical force on gene expression, the Dynamic Culture System (ATMS Boxer™, TAIHOYA Corporation, Kaohsiung City, Taiwan) was used to subject the artificial ligaments to uniform uniaxial stretch, with the stretching parameters set to a 1 Hz rate, 10 % strain and 2 h/d for a period of 7 d. MSCs were seeded on profiled fibre PET artificial ligaments at $6 \times 10^5$ cells/cm$^2$. Following 3 d of incubation, each PET structure was stretched by the dynamic culture system. After stretching for 7 d, cells were harvested to characterise gene expression by RT-qPCR.

**ALP assay**

The ALP activity assay was performed on day 7 and 14 of culture. ALP released from the cells into the medium was measured using a commercially available ALP assay kit (ab83369, Abcam). The medium was collected and added into a 96-well plate, each well of which contained 30 µL of the sample. 60 µL of ALP regent (5 mmol/L pNPP solution) were added to each well and incubated at 25 °C for 60 min. 20 µL of Stop Solution was added to each well to stop reaction. Then, the plate was read using

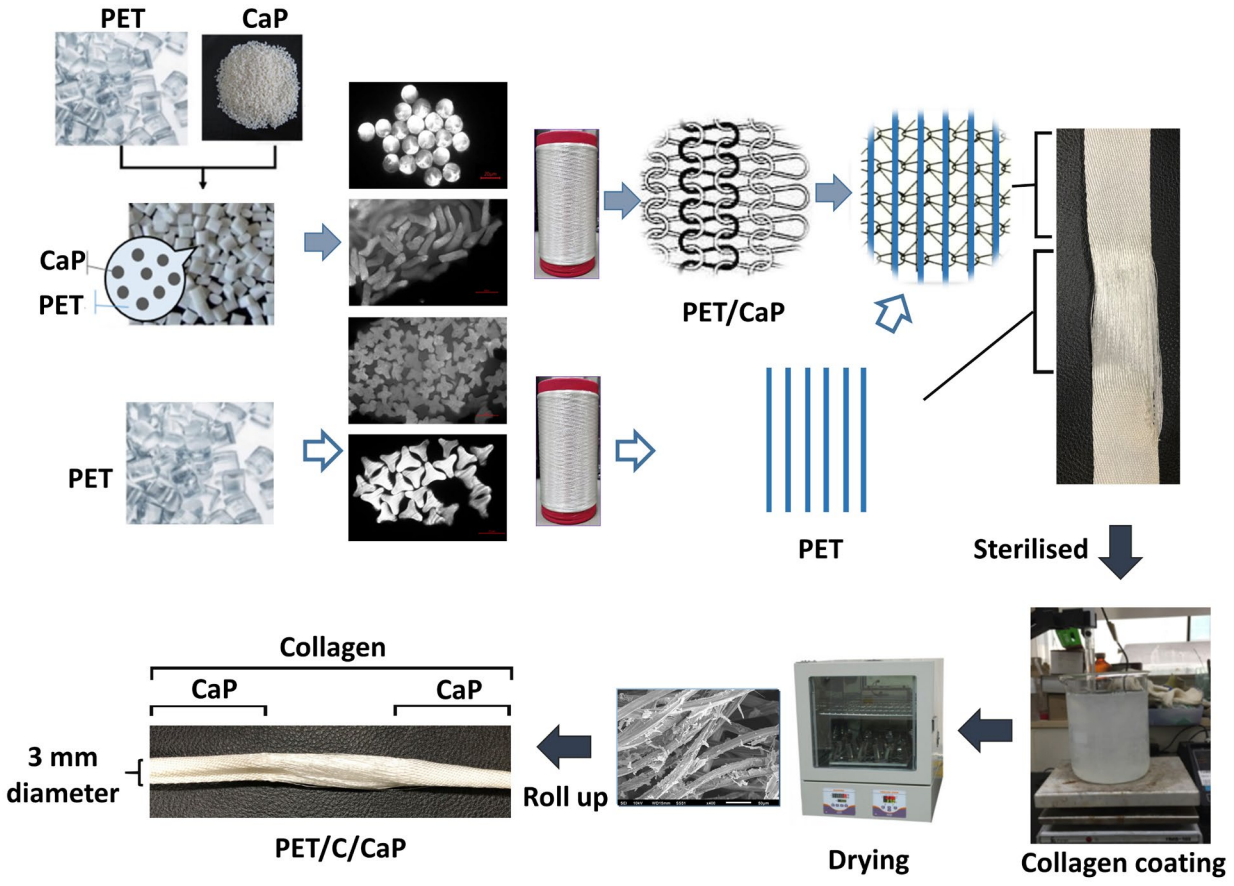


**Fig. 1. The production process of profiled PET/C/CaP artificial ligaments.**

**Table 1. RT-qPCR primer sequences.**

| Oligo name | Sequence (5′ to 3′) (forward: F; reverse: R) |
|---|---|
| *Scx* | F: TTGAGCAAAGACCGTGACAG<br>R: CTGTGCTCAGATCAGGTCCA |
| *Egr1* | F: TTATCCCAGCCAAACTACCC<br>R: CAGAGGAAGACGATGAAGCA |
| *Col1a1* | F: GGAAGAGCGGAGAGTACTGG<br>R: CATGCTCTCTCCAAACCAGA |
| *Col3a1* | F: AGGCCAATGGCAATGTAAAG<br>R: GGCCTTGCGTGTTTGATATT |
| *Tnc* | F: TGCCATGAAGGGATTTGAAGA<br>R: GGCTGTCAGAAGGCCAGATG |
| *Tnmd* | F: CCTCAGCAGTGGTCTCTCA<br>R: AAGGCCAGGATACCAAACAC |
| *Runx2* | F: AAGTGCGGTGCAAACTTTCT<br>R: AGGCTGTTTGACGCCATAGT |
| *OCN* | F: GGTGGTGAATAGACTCCGGC<br>R: AGCTCGTCACAATTGGGGTT |
| *OP* | F: AGCATTCTCGAGGAAGCCAG<br>R: AGTGTTTGCTGTAATGCGCC |
| *ALP* | F: CTACGCACCCTGTTCTGAGG<br>R: CCCAAGAGAGAAACCCACC |
| *GAPDH* | F: GTGGACCTCATGGCCTACAT<br>R: GGATGGAATTGTGAGGGAGA |

a spectrophotometer (Molecular Devices) at 405 nm absorbance.

**Alizarin red S staining**

To further examine the osteoinductive effects of CaP, the medium was changed into an osteogenic medium [containing 0.1 μmol/L dexamethasone, 50 μmol/L L-ascorbate-2-phosphate and 10 mmol/L β-glycerphosphate (Sigma-Aldrich)] and changed every 4 d. The alizarin red S staining assay was performed on predetermined days of culture to analyse the cell mineralisation. After removing the culture medium and fixing in 4 % paraformaldehyde in PBS (pH 7.4) for 15 min at room temperature, the samples were washed 3 times with ddH2O. Alizarin red S (40 mmol/L) was added to each well for 30 min. Cells were washed with $ddH_2O$ and the plates were photographed using a digital camera (Panasonic DMC-G7). For quantification of mineralisation, the bound stain was solubilised in 10 % (w/v) cetylpyridinium chloride (Sigma-Aldrich) in 10 mmol/L sodium phosphate at pH 7.0. Then, the extracted stain was transferred to a 96-well plate and measured using an ELISA reader at a wavelength of 562 nm.

**Animals and surgical procedures**

In accordance with national animal welfare legislation, the following animal study was approved by the Institutional Animal Care and Use Committee of Master Laboratory Co., Taiwan (approval number MI-201906-03). 24 New Zealand white rabbits (Master Laboratory Co., Ltd., Taipei City, Taiwan) with a mean body weight of 3.0 kg and an age of 6 months were selected. The animals received MCL reinforcement reconstruction of the hind limbs. One knee received the profiled PET/C/CaP graft, while the other a commercialised product (LARS®) as a control.

All surgical procedures were performed under general anaesthesia by intramuscular injection of a Zoletil®-Rompun® mixture (Zoletil® 15 mg/kg + Rompun® 0.05 mL/kg; Zoletil®, Virbac Taiwan, Taipei City, Taiwan; Rompun®, Bayer Taiwan, Taipei City, Taiwan). For analgesia, the rabbits were given meloxicam (0.15 mg/kg peroral; Metacam, Boehringer Ingelheim) 1 d pre-operatively, immediately pre-operatively and 2 d following surgery. During the operation, two tunnels were drilled in the tibial and femoral condyles. Using a guide pin to allow the PET structures to pass through the two tunnels, there was a button at the end of the PET structures. The end was an anchor at the lateral side of the tibial condyle tunnel and the medial femoral tunnel was locked using a titanium alloy ($Ti_6Al_4V$) interference screw (Tsai *et al.*, 2018). Finally, a half-incision was made on the MCL and sutured using a PET structure. The other leg underwent the same surgery but was implanted with LARS® as a control. Following surgery, the animals were returned to their cages and were allowed free movement without any restriction or

immobilisation of their extremities. Animals' physical and mental state and behaviour were assessed daily by observation and during interactions with the animal carer. An X-ray was taken after 1 month to check the position of the buttons and screws for graft stability. Rabbits were euthanised at 1 and 3 months to complete the subsequent experiments, including a μCT scan, histology, SEM and the material pull-out test.

**Histological analysis and SEM**

Tissue samples were carefully excised and fixed in 4 % paraformaldehyde in PBS (pH 7.4) for 2 h at room temperature, dehydrated through an alcohol gradient, embedded in paraffin-wax and sliced. For the histological examination, sections (7 μm) were stained with H&E and Masson's trichrome stain according to standard procedures. For morphological examination, SEM was used and the method was the same as that mentioned above (see SEM paragraph).

**μCT analysis**

The 6 stifle joints were harvested and scanned by μCT analysis (Skyscan 1176, Bruker) at each time point. High voltage scanning (90 kVp, 278 μA, at a 25 W output with a 360° scan) with an 18 μm sample size was used for the experiment. Image reconstruction was performed using the GPU-based reconstruction software GPU-Nrecon. Automatic threshold and structure densitometry analyses were performed using CTAn software (Bruker).

**Pull-out test**

A material testing machine (ElectroForce® 3510-AT, Bose Corporation-ElectroForce Systems Group, Eden Prairie, MN, USA) was used for biomechanical

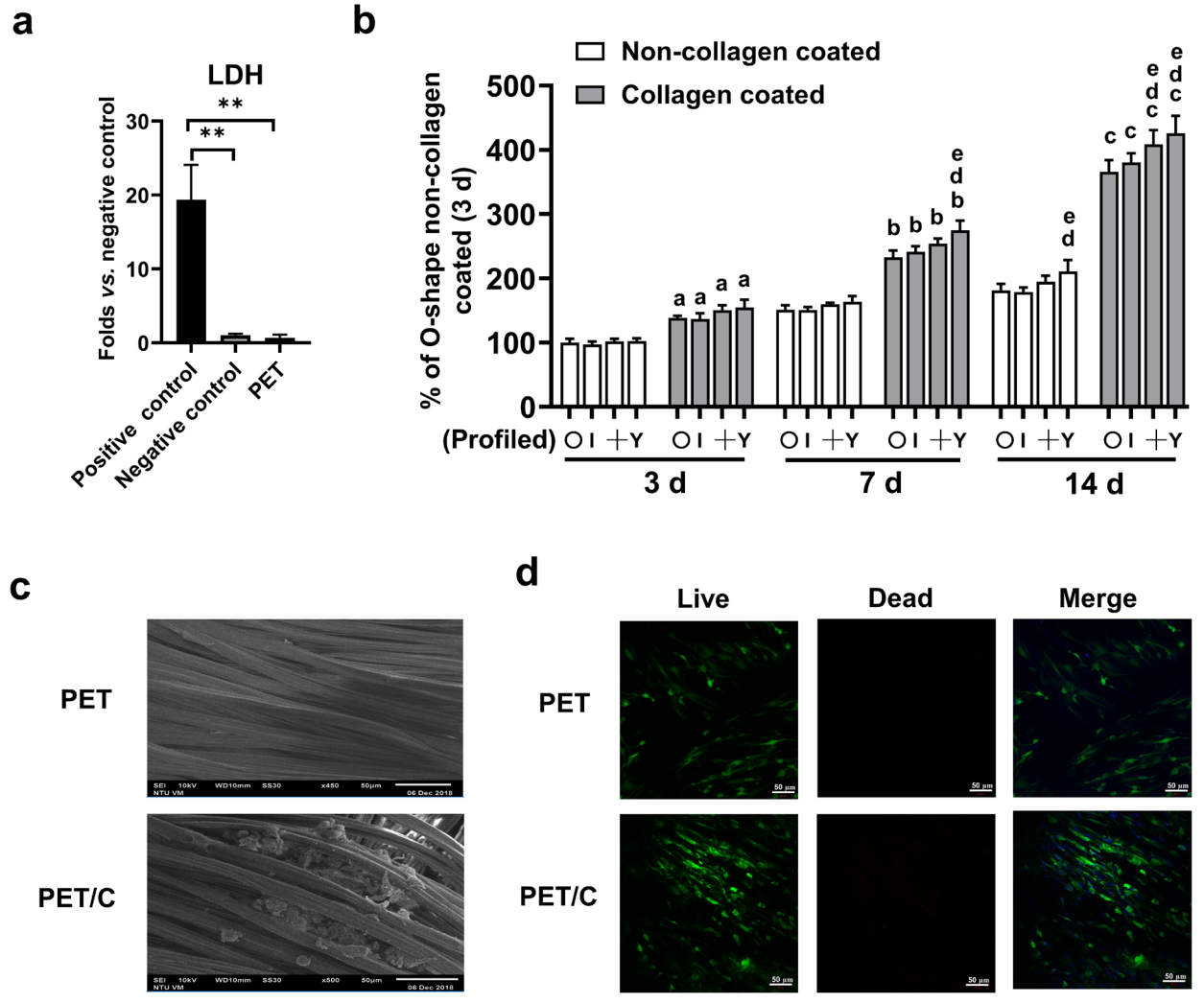


**Fig. 2. Biocompatibility of the profiled PET filaments.** (**a**) The LDH cytotoxicity test showed that the PET filaments did not cause cytotoxicity ($n = 8$; ** $p < 0.01$). (**b**) Cell viability assays were investigated at days 3, 7 and 14 to examine the effects of the different profiled filaments and collagen coating conditions upon cell proliferation ($n = 8$; [a,b,c] $p < 0.01$ compared to the same profiled filaments with or without collagen coating at day 3, 7 and 14, respectively; [d] $p < 0.01$ compared to the O-shaped filaments with identical coating conditions at the same time point; [e] $p < 0.01$ compared to the I-shaped filaments with identical coating conditions at the same time point). (**c**) Cells on the Y-shaped PET/C filaments showed better adhesion and growth than Y-shaped PET filaments by SEM after 7 d of culture. (**d**) Y-shaped PET/C group showed better cell growth in LIVE/DEAD assay than Y-shaped PET group after 14 d of culture.

testing. The test was performed at room temperature (25 °C) in a moist environment. Rabbit knee-joints were isolated and all periarticular soft tissues were removed except for the implanted PET structures or LARS®. The artificial ligament was cut from the screw end of the femur and the fixed button was cut off. The end of the free ligament and tibia bone were fixed onto the mechanical testing machine, allowing tensile loading along the axis of the implants at a strain rate of 0.5 mm/min. The machine continued elongation until the implants were pulled out and the maximal load was recorded.

**Statistical analysis**

All the data are expressed as the mean ± SD. To evaluate the differences between two groups, an independent *t*-test was performed and, for comparisons between three or four groups, one-way

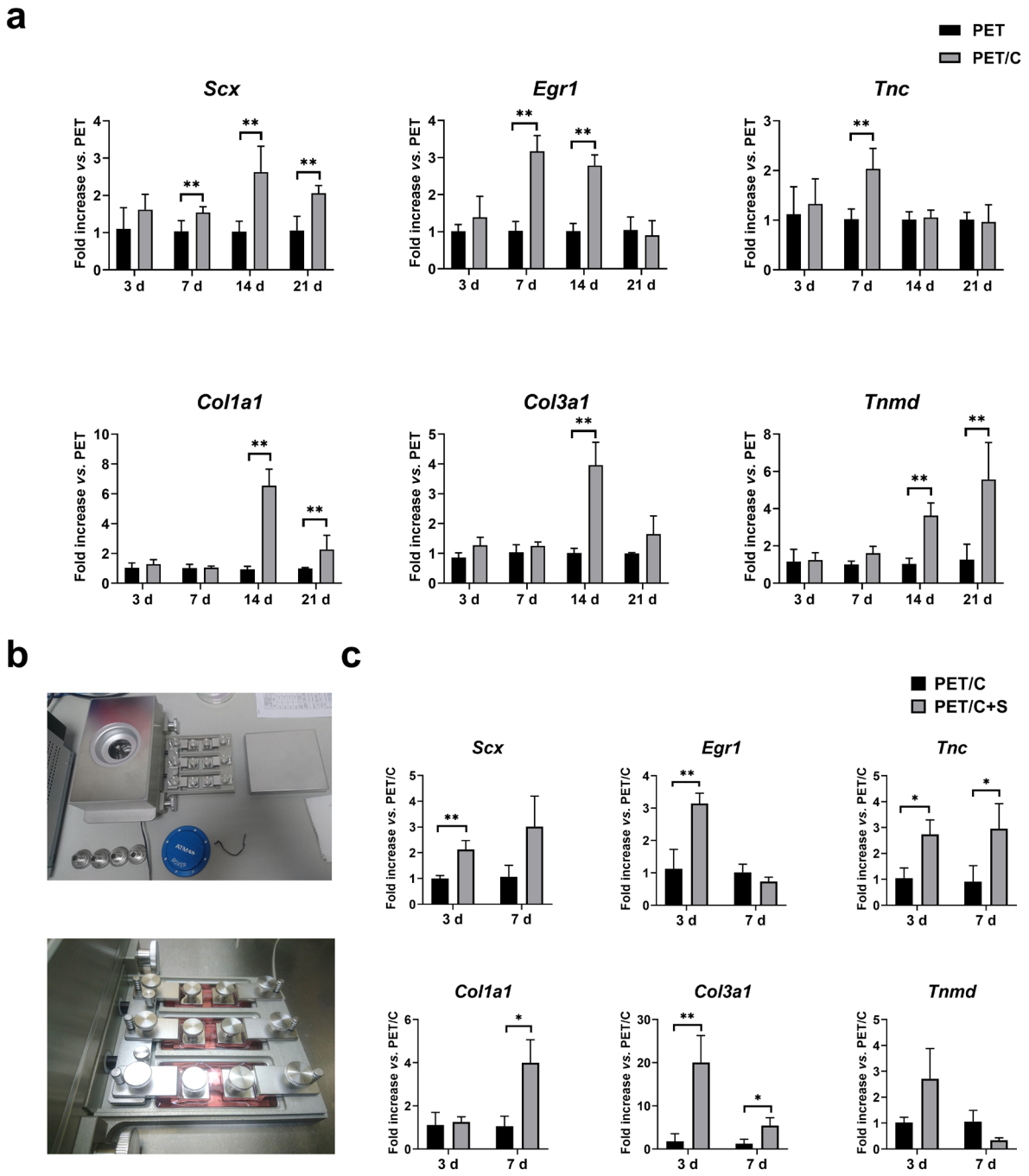


**Fig. 3. Effects of collagen coating and mechanical stretching on the expression of tendon/ligament-related markers.** (**a**) PET/C filaments significantly increased the expression of the tendon/ligament-related markers *Scx*, *Egr1*, *Tnc*, *Tnmd*, *Col1a1* and *Col3a1* at certain time points ($n = 6$; ** $p < 0.01$). (**b**) The dynamic tissue-loading culture system used. (**c**) MSCs were cultured on the PET/C filaments for 3 d and then treated with a 2 h session of 1 Hz, 10 % elongation mechanical stretch for the following 3 or 7 consecutive days. The expression levels of the tendon/ligament-related markers *Scx*, *Egr1*, *Tnc*, *Tnmd*, *Col1a1* and *Col3a1* were measured by qRT-PCR ($n = 6$; ** $p < 0.01$, * $p < 0.05$).

ANOVA was performed. $p < 0.05$ was considered statistically significant.

## Results

### Biocompatibility of the profiled PET filaments

The LDH cytotoxicity test showed that the PET filaments did not cause cytotoxicity (Fig. 2**a**). To examine the effects of the different profiled filaments and collagen coating conditions upon cell proliferation, MSCs were cultured on four different profiled PET filaments with or without collagen coating and cell viability assays were investigated at each time point. At days 3, 7 and 14, PET/C (collagen-coated PET) filaments significantly promoted cell proliferation more than PET (non-collagen coated) filaments. In PET filaments, the Y-shaped group significantly promoted cell proliferation, more than the O- and I-shaped groups, respectively, at day 14. In PET/C filaments, the Y-shaped group significantly promoted cell proliferation more than the O- and I-shaped groups, respectively, at day 7. In addition, Y- and +-shaped groups showed significantly increased cell proliferation compared with the O- and I-shaped groups, respectively, at day 14 (Fig. 2**b**). SEM was used to observe the adhesion and growth of MSCs on profiled PET and PET/C filaments. Cells on the profiled PET/C filaments showed better adhesion and growth than profiled PET filaments after 7 d of culture (Fig. 2**c**). The PET/C group also showed better cell growth in a LIVE/DEAD assay than the PET group after 14 d of culture (Fig. 2**d**). In summary, a Y-shaped profiled filament promoted cell growth better than other groups and collagen-coating helped with cell adhesion and growth. Based on the above experimental results, the Y-shaped profiled filaments were used for subsequent experiments.

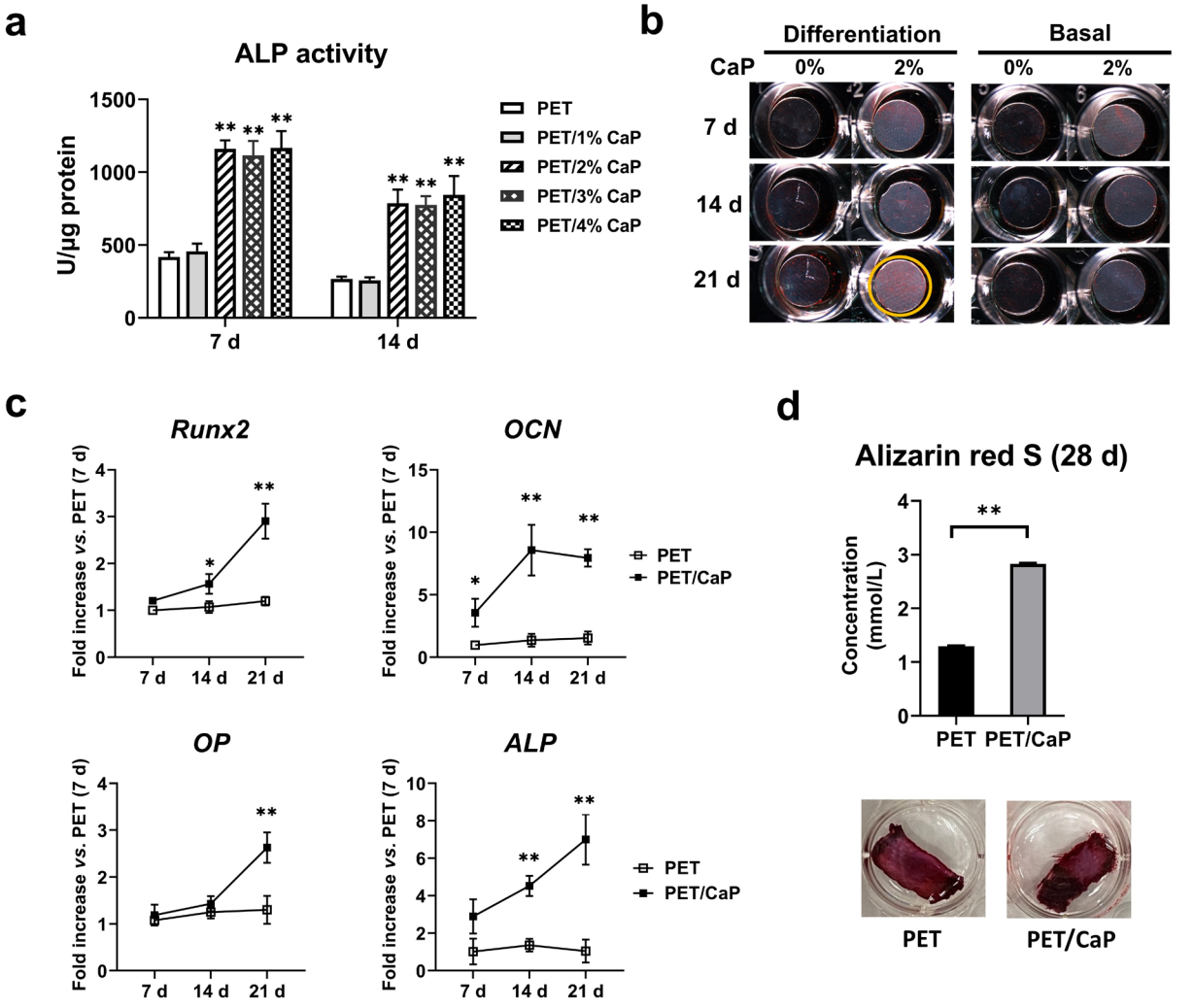


**Fig. 4. PET/CaP filaments enhanced osteogenesis of MSCs.** (**a**) MSCs cultured on 2 %, 3 % and 4 % w/w PET/CaP filaments significantly increased ALP activity as compared with PET group ($n = 8$; ** $p < 0.01$). (**b**) MSCs were cultured with 2 % CaP and osteogenic medium for 7, 14 and 21 d, and alizarin red S staining showed that 2 % CaP with osteogenic medium enhanced mineralisation. (**c**) MSCs on PET/CaP fibres (2 % w/w) significantly enhanced *OCN* expression at day 7, *Runx2* and *OCN* expression at day 14 as well as *Runx2*, *OCN*, *OP* and *ALP* expression at day 21 under osteogenic medium culture ($n = 6$; * $p < 0.05$, ** $p < 0.01$). (**d**) Alizarin red S staining of MSCs on PET/CaP fibres showed significantly enhanced mineralisation at 28 d ($n = 3$; ** $p < 0.01$).

**Effects of collagen coating and mechanical stretching on the expression of tendon/ligament-related markers**

To examine the effects of collagen coating upon the expression of tendon/ligament-related markers, the mRNA levels of *Scx*, *Egr1*, *Tnc*, *Tnmd*, *Col1a1* and *Col3a1* were analysed by qRT-PCR. Compared to the PET filaments, MSCs on the PET/C filaments significantly increased the gene expression of the tendon/ligament-related transcription factors *Scx* and *Egr1* at day 7 (1.54 ± 0.16 and 3.17 ± 0.43, $p < 0.01$, respectively) and 14 (2.69 ± 0.69 and 2.78 ± 0.29, $p < 0.01$, respectively), while the expression of *Scx* remained high until day 21 (2.06 ± 0.21, $p < 0.01$). Next, the gene expression level of downstream matrix molecules was examined. Compared to the PET filaments, MSCs on the PET/C filaments showed significantly increased expression of matrix molecule genes, including *Tnc* at day 7 (2.03 ± 0.41, $p < 0.01$), *Col1a1* and *Col3a1* at day 14 (6.55 ± 1.11 and 3.96 ± 0.77, $p < 0.01$, respectively), as well as *Tnmd* at day 14 (3.63 ± 0.68, $p < 0.01$) and 21 (5.57 ± 1.98, $p < 0.01$) (Fig. 3**a**).

To mimic the *in vivo* loading conditions, a dynamic tissue-loading culturing system (ATMS BoxerTM, TAIHOYA Corporation, Taiwan) was used to examine the ligamentous differentiation of MSCs on PET/C filaments (Fig. 3**b**). MSCs were cultured on the PET/C filaments for 3 d and then treated with a 2 h session of 1 Hz, 10 % elongation mechanical stretch for the following 3 or 7 consecutive days. The results showed that mechanical stretching significantly increased *Scx* (2.13 ± 0.34, $p < 0.01$), *Egr1* (3.15 ± 0.31, $p < 0.01$), *Tnc* (2.71 ± 0.56, $p < 0.05$) and *Col3a1* (20.08 ± 6.2, $p < 0.01$) expression after 3 d compared to the non-stretched group. After 7 d of stretching, the expression levels of *Tnc* (2.96 ± 0.97, $p < 0.05$), *Col1a1* (3.99 ± 1.07, $p < 0.05$) and *Col3a1* (5.43 ± 1.84, $p < 0.05$) were significantly higher than those in the non-stretched group (Fig. 3**c**). *Tnmd* expression in stretched PET/C filaments was higher than in non-stretched PET/C filaments after 3 d of stretching and then decreases after 7 d. *Tnmd* expression level was variable and the differences between groups were not statistically significant.

**PET/CaP filaments enhanced osteogenesis of MSCs**

ALP is a marker of early maturation and differentiation of osteoblasts. To determine the proper mixing concentration of CaP, the CaP bioceramic was predispersed, mixed with PET at five different mass percentage concentrations (0 %, 1 %, 2 %, 3 % or 4 % w/w) to make the PET/CaP filaments. MSCs were cultured on the PET/CaP filaments for 7 and 14 d and

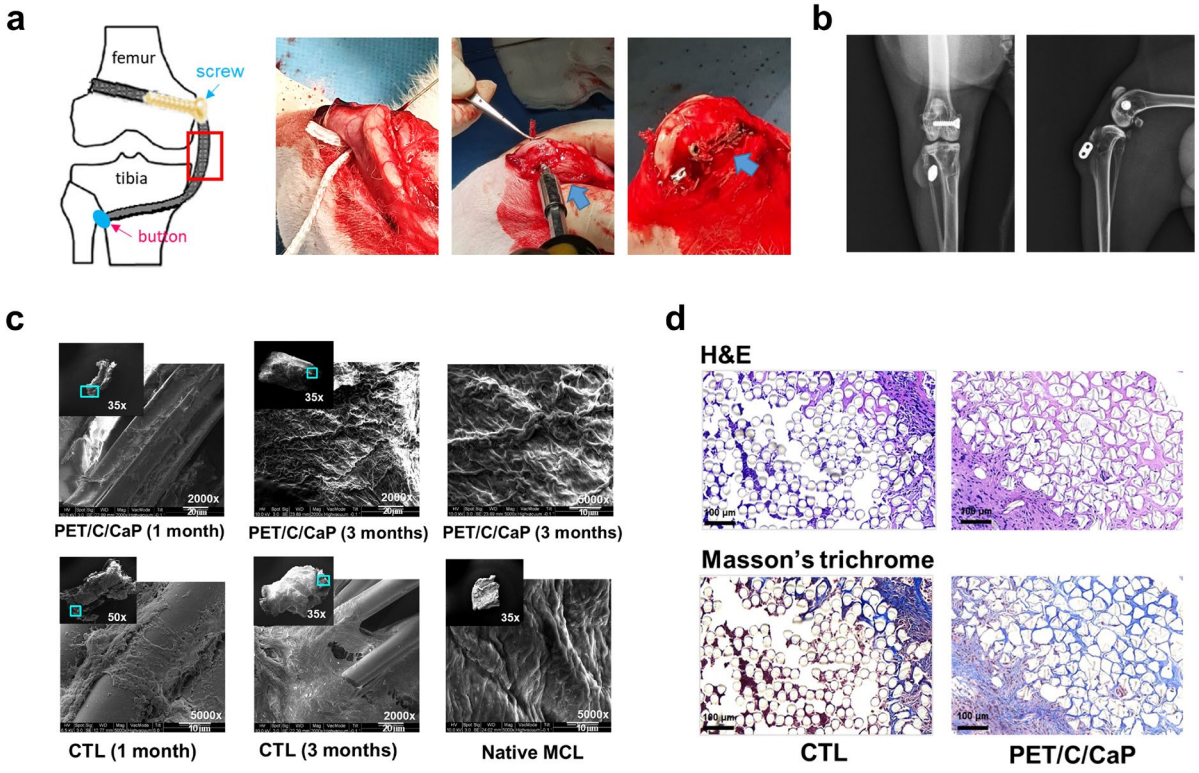


**Fig. 5. The PET/C/CaP graft enhanced cell growth and ligamentous matrix remodelling.** (**a**) The animals received MCL reinforcement reconstruction of the hind limbs and the two ends of artificial ligaments were fixed with metal buttons and screws. (**b**) X-ray images taken 1 month post-operation showed that the graft fixation was stable. (**c**) Characterisation of the artificial ligaments by SEM was performed after 1 and 3 months and showed that the ligaments in the PET/C/CaP group had structural features similar to those of native ligament tissues at 3 months. (**d**) H&E (upper row) and Masson's trichrome (lower row) staining at 3 months showed the growth of the collagen matrix in the PET/C/CaP group was significantly better than that in the control group (LARS®). CTL: control.

the result showed 2 %, 3 % and 4 % w/w PET/CaP filaments significantly increased ALP activity more than the PET group (Fig. 4**a**). 2 % CaP was selected for further investigation to enhance osteogenesis, as 2 % CaP significantly increased ALP activity while increasing concentrations to 3 % or 4 % CaP had no further effect (Fig. 4**a**). To further examine the osteoinductive effects of CaP, MSCs were cultured with osteogenic medium for 7, 14 and 21 d. Alizarin red staining showed that 2 % CaP with osteogenic medium significantly enhanced mineralisation (Fig. 4**b**). Compared to PET filaments, MSCs cultured on the PET/CaP filaments (2 % w/w) significantly enhanced *OCN* ($p < 0.05$) expression at day 7, *Runx2* ($p < 0.05$) and *OCN* ($p < 0.01$) expression at day 14 and *Runx2* ($p < 0.05$), *OCN* ($p < 0.01$), *OP* ($p < 0.01$) and *ALP* ($p < 0.01$) expression at day 21 under osteogenic medium culture (Fig. 4**c**). Alizarin red S staining of the MSCs on the PET/CaP filaments also showed significantly enhanced mineralisation after

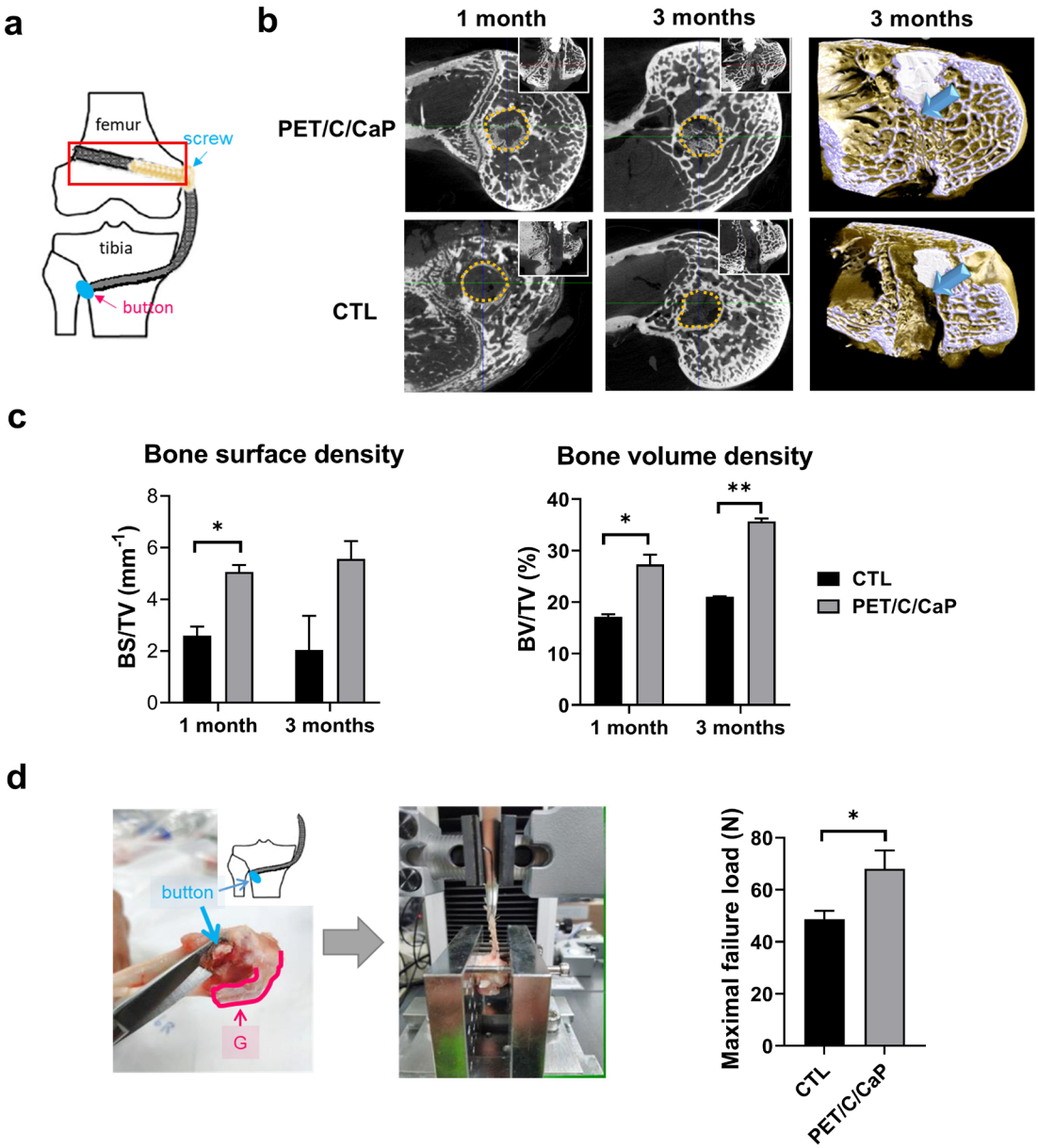


**Fig. 6. The PET/C/CaP graft enhanced bone formation and graft pull-out load *in vivo*.** (**a**) The medial femoral tunnel was locked using a titanium alloy (Ti6Al4V) interference screw. (**b**) The μCT analysis showed that bone formation in the PET/C/CaP group was better than in the control group 1 and 3 months post-operation. 3D μCT demonstrated that the bone tunnel in the PET/C/CaP group had completely healed after 3 months. (**c**) The bone surface density of the PET/C/CaP group at 1 month (5.06 ± 0.28 $mm^{-1}$) was significantly higher than that of the control group (2.60 ± 0.36 $mm^{-1}$). The bone volume density of the PET/C/CaP group after 1 (27.32 ± 1.88 %) and 3 months (35.67 ± 0.60 %) was significantly higher than that of the control group (17.14 ± 0.50 % and 21.06 ± 0.05 %, respectively) ($n = 3$, * $p < 0.05$, ** $p < 0.01$). (**d**) The ultimate pull-out load of the constructs was analysed by a material testing machine. The maximal pull-out failure load of the PET/C/CaP group at 3 months (68 ± 7.07 N) was significantly higher than that of the control group (48.67 ± 3.21 N) ($n = 3$, * $p < 0.05$). CTL: control.

28 d (2.827 ± 0.021 mmol/L in the PET/CaP group *vs.* 1.297 ± 0.015 mmol/L in the PET group, $p < 0.01$) (Fig. 4**d**).

**PET/C/CaP graft enhanced cell growth and ligamentous matrix remodelling *in vivo***

The animal study was conducted to evaluate the effect of profiled PET/C/CaP ligament in a rabbit knee MCL reinforcement reconstruction model and the two ends of artificial ligaments were fixed using metal buttons and screws (Fig. 5**a**). X-ray images that were taken 1 month post-operation showed that the graft fixation was relatively stable. Both the buttons and screws remained in their original surgical positions (Fig. 5**b**). SEM showed no significant difference in morphology between the PET/C/CaP group and the control group (LARS®) 1 month post-operation. 3 months after surgery, SEM showed that the ligaments in the PET/C/CaP group had structural features similar to those of native ligament tissue. In contrast, the ligaments in the control group had no apparent extracellular matrix adaptive changes (Fig. 5**c**). H&E and Masson's trichrome staining at 3 months showed that cells and collagen matrix in the PET/C/CaP group were filled among the artificial ligament fibres, whereas the number of cells and amount of collagen matrix in the control group was small and distributed only around the artificial ligament (Fig. 5**d**). The results revealed that the PET/C/CaP graft enhanced cell growth and ligamentous matrix remodelling.

**PET/C/CaP graft enhanced bone formation and graft pull-out load *in vivo***

The medial femoral tunnel was locked using a titanium alloy (Ti6Al4V) interference screw (Fig. 6**a**). The μCT scans 1 and 3 months post-operation showed that bone formation in the PET/C/CaP group was better than in the control group (LARS®). 3D μCT also showed that the bone tunnel in the PET/C/CaP group had totally healed after 3 months (Fig. 6**b**). The bone surface density of the PET/C/CaP group at 1 month (5.06 ± 0.28 $mm^{-1}$, $p < 0.05$) was significantly higher than that of the control group (2.60 ± 0.36 $mm^{-1}$). The bone volume density of the PET/C/CaP group at 1 (27.32 ± 1.88 %, $p < 0.05$) and 3 months (35.67 ± 0.60 %, $p < 0.01$) was significantly higher than that of the control group (17.14 ± 0.50 % and 21.06 ± 0.05 %, respectively) (Fig. 6**c**). The maximal pull-out failure load of the PET/C/CaP group at 3 months (68 ± 7.07 N, $p < 0.05$) was significantly higher than that of the control group (48.67 ± 3.21 N) (Fig. 6**d**). Results indicated that a PET/C/CaP graft enhanced bone formation in a bone tunnel and graft pull-out failure load.

## Discussion

The PET/C/CaP ligament demonstrated good biocompatibility, ligamentisation and ligament-bone healing following knee MCL reinforcement reconstruction. From the cross-sectional filament profile perspective, the Y- and +-shaped profiled filaments had better cell proliferation than the O-shaped group, especially the Y-shaped filaments. A previous study indicated that scaffolds with a higher surface-area-to-volume ratio increase cell attachment and proliferation (Chen *et al.*, 2009). Noncircular-shaped fibres provide a higher surface-area-to-volume ratio than those with round cross sections (Park *et al.*, 2013; Yeom and Pourdeyhimi, 2011). Park *et al.* (2013) designed fibres with circular, triangular and cruciform cross sections on biodegradable PCL. The results showed that the cruciform-shaped fibre exhibited the most remarkable improvement in cell proliferation: twice as high as that of the circular fibre after 1 week, followed by the triangular fibre and the circular fibre as the last. Secretion of the extracellular matrix was also more significant on the cruciform shape than on the circular shape. The gaps between the PCL fibres were remarkably filled with cells between the cruciform fibres (Park *et al.*, 2013). In addition to providing a higher surface-area-to-volume ratio than those with round cross sections, the profiled cross section fibres used in the present study had the characteristics of moisture-wicking fibres, which could help with the circulation of fluids through capillary action. Hence, they were more conducive to cell growth. In cell growth experiments, in the presence or absence of collagen coating, Y-shaped-profile filament promoted cell growth better than other groups, so the Y-shaped-profile filaments were used in the subsequent filament profile design.

PET is a hydrophobic material. Scaffolds coated with collagen improve their affinity for water, cell attachment, proliferation, migration and ligamentisation (Silva *et al.*, 2020). Poly(ethylene-co-vinyl alcohol) immobilised with collagen exhibits enhanced cell proliferation and leads to a shorter cell doubling time than that in tissue culture dishes (Matsumura *et al.*, 2004). Poly(L-lactide) scaffolds coated with type I collagen show higher cell viability, greater cell infiltration depth into the scaffold fibres and a higher cell infiltration ratio than scaffolds coated with fibronectin or both fibronectin and collagen (Chang *et al.*, 2020). ACL-derived fibroblasts cultured on a scaffold made of collagen display higher *Tnmd* and type I collagen expression than those cultured on an elastin scaffold, suggesting that collagen could induce ligamentisation to a greater extent than elastin (Mizutani *et al.*, 2014). An animal study using polydioxanone coated with collagen and elastin displayed a higher load from the pull-out test and more tissue regeneration at the insertion site of the rabbit MCL following implantation for 6 weeks (Hirukawa *et al.*, 2018).

The present study found that PET with a collagen coating increased MSC proliferation, ligament-related gene expression and extracellular matrix content. SEM results indicated that the cells clustered on the surface of collagen-coated PET. The larger

number of cells on collagen-coated PET than on uncoated PET scaffolds indicated that collagen's presence affected cell response positively. The ligament-related transcription factors *Scx* and *Egr1* had higher expression after 7 d of culture with PET/C than PET. Other tendon matrix markers, *Col1a1*, *Col3a1* and *Tnmd*, showed higher expression in the PET/C group after 2 weeks. These results showed that collagen could induce ligamentous differentiation of MSCs in the early stage. SEM observations 3 months after implantation demonstrated that more cells or extracellular matrix filled the gaps of the profiled PET/C/CaP ligament than the control. Histological findings also showed that more tissue occupied the space between the profiled PET/C/CaP ligament than the commercial artificial ligament. Surface modification of collagen on the profiled PET/C/CaP ligament indeed resulted in better cell growth and ligamentisation.

To simulate a ligament's *in vivo* loading conditions, a cyclic stretching device was used, a 3D environment designed for cell growth and the ligamentous differentiation of MSCs observed under mechanical stimulation. Under mechanical stimulation, cells play an active role in regulating extracellular matrix secretion and interacting with external force and hormone factors (Wang, 2006). Notably, the 2D tensile model cannot fully mimic 3D stretching, which is more physiologically relevant (Wang *et al.*, 2018b). However, the parameters were set differently in the 3D models due to the mechanical properties of the selected raw materials, cell culture strategies and customised bioreactors. One study manufactured a 3D collagen scaffold using adipose-derived stem cells and applied a cyclic uniaxial tensile stretch, aiming to determine the optimal parameters for tenogenesis (Subramanian *et al.*, 2017). The results suggested that 2 % strain and 0.1 Hz were the best parameters for tenogenesis without cross-differentiation effects. A report selecting 10 % strain and 0.5 Hz for 60 min to stretch cells embedded in a PEGylated-fibrinogen scaffold showed higher collagen gene expression and improved mechanical properties (Testa *et al.*, 2017). Another study showed that under 6 % strain, 0.25 Hz and 8 h of stress/d, uniaxial loading demonstrated better tenogenic-specific differentiation of scaffold-free tendon-derived stem cells in a 3D environment than in a static 3D culture (Wang *et al.*, 2018c). ACL-derived fibroblasts seeded onto the poly(L-lactide) 3D scaffold with 2 % or 5 % strain and 1 Hz displayed upregulation of collagen types I and III, fibronectin and tenascin C gene expression (Kreja *et al.*, 2012). Consequently, a customised bioreactor was used, with cells cultured onto the collagen-coated artificial ligament and fixed onto the clamps at both ends of the bioreactor. The strain rate was set at 10 % and the frequency of 1 Hz for 2 h/d imitated the regular cadence and moderate-to-vigorous physical activity of healthy adults (Tudor-Locke *et al.*, 2019; 2011). The results suggested that mechanical stretching promoted the ligamentous differentiation of MSCs on PET/C filaments *in vitro*, which may suggest that the artificial ligament in this experiment contributed to the cell ligamentous differentiation and tissue ligamentisation under the mechanical environment.

This study used a pre-dispersed CaP bioceramic mixed with PET pellets through spinning to make the PET/CaP filaments. This is a different protocol from previous research, which mainly used coating or electrodepositing CaP on PET artificial ligaments. Results indicated that MSCs cultured on the PET/CaP (2 % w/w) filaments had significantly enhanced *Runx2*, *OCN*, *OP* and *ALP* expression, ALP activity and Ca deposition *in vitro*. Li *et al.* (2011) explored the osseointegration of HA-coated PET artificial ligaments. The results showed that HA coating elevates *OP* and collagen I mRNA expression and induces new bone formation, indicating that HA coating effectively promoted osseointegration. However, HA powder agglomerates on the surface of the PET artificial ligament material, which affects the size effect of HA (Li *et al.*, 2011). In the present study, the hybrid spinning process of CaP and PET prevented HA from forming agglomerates on the PET surface. A recent study by Wang *et al.* (2018a), using the plasma spraying technique to make PET/HA films (PET/HA-plasma), effectively coated HA on a PET material and promoted the growth of BMSCs on this PET material. BMSCs grown on the PET/HA-plasma showed upregulated mRNA expression of *BMP-2*, *VEGF*, *OCN* and *eNOS in vitro*. The biomechanical strength of the bone-graft complex with PET/HA-plasma was also improved *in vivo* (Wang *et al.*, 2018a). The results of the present study were consistent with previous studies regarding promotion of osteogenesis.

The present animal study found that the profiled PET/C/CaP ligament had more matrix deposition than the control group. More cells and cell matrix could be detected followin H&E histology and Masson's trichrome staining. In a previous study, layer-by-layer coatings of hyaluronic acid and cationised gelatine on PET artificial ligament grafts significantly enhanced cell adhesion and facilitated cell growth relative to a pure PET graft *in vitro*. Furthermore, *in vivo* study also demonstrated that there was much more formation of type I collagen in the hyaluronic acid-cationised gelatine coating PET group than in the pure PET group in a rabbit and porcine ACL-reconstruction model (Li *et al.*, 2012). Gelatine is known as hydrolysed collagen. Collagen coating and gelatine have a similar function for cell attachment and biocompatibility. In the present *in vivo* study, the profiled PET/C/CaP ligament showed good cell proliferation and ligamentisation. Wang *et al.* (2018d) used LARS® combined with an autograft ligament implanted as a reconstructed ACL and compared it with the autograft reconstructor only. In that study, rabbits were used as an animal model and LARS® combined with an autograft ligament had an

effect similar to that of the autograft reconstructors. There were no significant side effects and satisfactory biointegration was observed in both groups. The present study used collagen-coated PET, which has a design similar to an autograft tendon combined with artificial structures without cells.

Cell composite structures or combinations with autotissue could be considered in future material designs (Wang *et al.*, 2018d). Regarding osteointegration, μCT showed that the profiled PET/C/CaP ligament had good osteogenesis and bone density. Jin *et al.* (2016) implanted hydroxyapatite- and HA/BMP-coated fibres into rabbit femora. They found that the HA- and BMP-coated groups had good osteoinductive ability for MSCs and good osteogenesis in rabbits (Jin *et al.*, 2016). In the present study, the profiled PET/C/CaP ligament showed better osteogenesis than the control group, also observed in the pull-out test.

Although the surface adjustment of the PET ligament provides several advantages to improve the biocompatibility and tissue regeneration neighbouring the graft, there are still some limitations to this material. PET is non-degradable and the histology was performed over fewer than 3 months. Whether the artificial ligament would wear out over several years of usage, causing synovitis or inflammation within the articular space, is unknown. Future studies should prolong the test period to determine the strengths and drawbacks of this synthetic graft. To minimise the sacrifice of animals, the grafts were implanted into both knees of the rabbits. The usual care was provided and the animals were allowed to return to cage activity following surgery; however, it was possible that the bilateral knee injury caused the rabbits to have intense pain, a decreased willingness to move and a lowered appetite. The pain condition was significantly improved through the administration of analgesics. Although no animal died from excessive stress, to improve their well-being, future animal studies should treat one limb at a time. In the present study, the artificial ligament was implanted as a MCL augmentation device, owing to the availability and ease of approach. However, the prevalence rate of ACL tears is higher in the clinic and intra-articular healing is much more challenging due to insufficient nutrition and circulation. The effects of utilising this artificial ligament for ACL replacement should be investigated in the future. Last but not least, the results from the animal study may not be completely in accordance with those applied to humans; therefore, clinicians must consider both the benefits and disadvantages before performing ligament repair or reconstruction surgery.

In conclusion, the profiled PET/C/CaP ligament was developed for enhancing cell growth, ligamentisation and ligament-bone healing. The *in vitro* study revealed that the profiled PET/C filaments improved cell proliferation and cell attachment and induced the ligamentous differentiation of MSCs. Furthermore, the profiled PET/CaP filaments enhanced osteogenic gene expression, ALP activity and mineralisation of MSCs. The *in vivo* study in a rabbit knee MCL reinforcement reconstruction model indicated that the profiled PET/C/CaP ligament enhanced ligamentous matrix remodelling and bone formation. This new design is an effective strategy and can be considered as an optional ligament augmentation device or synthetic graft for ligament reconstruction. As the design exhibited promising results, future studies can include more animals to confirm the long-term effects of intra-articular ligament reconstruction.

## Acknowledgments

We are grateful for the technical support provided by the staffs of the P2 Lab of the Orthopaedics Department, and the Microscopy Core Facility, Department of Medical Research, National Taiwan University Hospital. We also thank the staffs of the Taiwan Textile Research Institute for their technical support in artificial ligament manufacturing.

## References

Bashaireh KM, Audat Z, Radaideh AM, Aleshawi AJ (2020) The effectiveness of autograft used in anterior cruciate ligament reconstruction of the knee: surgical records for the new generations of orthopedic surgeons and synthetic graft revisit. Orthop Res Rev **12**: 61-67.

Bollen S (2000) Epidemiology of knee injuries: diagnosis and triage. Br J Sports Med **34**: 227-227.

Cai J, Wan F, Dong Q, Jiang J, Ai C, Sheng D, Jin W, Liu X, Zhi Y, Wang S, Sun Y, Chen J, Shao Z, Chen S (2018) Silk fibroin and hydroxyapatite segmented coating enhances graft ligamentization and osseointegration processes of the polyethylene terephthalate artificial ligament *in vitro* and *in vivo*. J Mater Chem B **6**: 5738-5749.

Cai J, Zhang Q, Chen J, Jiang J, Mo X, He C, Zhao J (2021) Electrodeposition of calcium phosphate onto polyethylene terephthalate artificial ligament enhances graft-bone integration after anterior cruciate ligament reconstruction. Bioact Mater **6**: 783-793.

Chang CW, Lee JH, Chao PHG (2020) Chemical optimization for functional ligament tissue engineering. Tissue Eng Part A **26**: 102-110.

Chen C, Li H, Guo C, Chen S (2016) Preparation and *in vitro* evaluation of a biomimetic nanoscale calcium phosphate coating on a polyethylene terephthalate artificial ligament. Exp Ther Med **12**: 302-306.

Chen M, Patra PK, Lovett ML, Kaplan DL, Bhowmick S (2009) Role of electrospun fibre diameter and corresponding specific surface area (SSA) on cell attachment. J Tissue Eng Regen Med **3**: 269-279.

Dong C, Lv Y (2016) Application of collagen scaffold in tissue engineering: recent advances and new perspectives. Polymers (Basel) **8**: 42. DOI: 10.3390/polym8020042.

Höher J, Scheffler S, Weiler A (2003) Graft choice and graft fixation in PCL reconstruction. Knee Surg Sports Traumatol Arthrosc **11**: 297-306.

Hirukawa M, Katayama S, Sato T, Inoue K, Niwa K, Ito N, Hattori T, Hosoi T, Unno H, Suzuki Y, Hasegawa M, Miyamoto K, Horiuchi T (2018) Development of a tissue-engineered artificial ligament: reconstruction of injured rabbit medial collateral ligament with elastin-collagen and ligament cell composite artificial ligament. Artif Organs **42**: 736-745.

Jin SK, Lee JH, Hong JH, Park JK, Seo YK, Kwon SY (2016) Enhancement of osseointegration of artificial ligament by nano-hydroxyapatite and bone morphogenic protein-2 into the rabbit femur. Tissue Eng Regen Med **13**: 284-296.

Kreja L, Liedert A, Schlenker H, Brenner RE, Fiedler J, Friemert B, Dürselen L, Ignatius A (2012) Effects of mechanical strain on human mesenchymal stem cells and ligament fibroblasts in a textured poly(L-lactide) scaffold for ligament tissue engineering. J Mater Sci Mater Med **23**: 2575-2582.

Lee SW, Hahn BD, Kang TY, Lee MJ, Choi JY, Kim MK, Kim SG (2014) Hydroxyapatite and collagen combination-coated dental implants display better bone formation in the peri-implant area than the same combination plus bone morphogenetic protein-2-coated implants, hydroxyapatite only coated implants, and uncoated implants. J Oral Maxillofac Surg **72**: 53-60.

Li H, Chen C, Zhang S, Jiang J, Tao H, Xu J, Sun J, Zhong W, Chen S (2012) The use of layer by layer self-assembled coatings of hyaluronic acid and cationized gelatin to improve the biocompatibility of poly(ethylene terephthalate) artificial ligaments for reconstruction of the anterior cruciate ligament. Acta Biomater **8**: 4007-4019.

Li H, Ge Y, Wu Y, Jiang J, Gao K, Zhang P, Wu L, Chen S (2011) Hydroxyapatite coating enhances polyethylene terephthalate artificial ligament graft osseointegration in the bone tunnel. Int Orthop **35**: 1561-1567.

Majewski M, Susanne H, Klaus S (2006) Epidemiology of athletic knee injuries: a 10-year study. Knee **13**: 184-188.

Matsumura K, Hyon SH, Nakajima N, Iwata H, Watazu A, Tsutsumi S (2004) Surface modification of poly(ethylene-co-vinyl alcohol): hydroxyapatite immobilization and control of periodontal ligament cells differentiation. Biomaterials **25**: 4817-4824.

Meng HW, Chien EY, Chien HH (2016) Dental implant bioactive surface modifications and their effects on osseointegration: a review. Biomark Res **4**: 24. DOI: 10.1186/s40364-016-0078-z.

Mizutani N, Kageyama S, Yamada M, Hasegawa M, Miyamoto K, Horiuchi T (2014) The behavior of ligament cells cultured on elastin and collagen scaffolds. J Artif Organs **17**: 50-59.

Overmann AL, Forsberg JA (2020) The state of the art of osseointegration for limb prosthesis. Biomed Eng Lett **10**: 5-16.

Park SJ, Lee BK, Na MH, Kim DS (2013) Melt-spun shaped fibers with enhanced surface effects: fiber fabrication, characterization and application to woven scaffolds. Acta Biomater **9**: 7719-7726.

Satora W, Królikowska A, Czamara A, Reichert P (2017) Synthetic grafts in the treatment of ruptured anterior cruciate ligament of the knee joint. Polim Med **47**: 55-59.

Silva M, Ferreira FN, Alves NM, Paiva MC (2020) Biodegradable polymer nanocomposites for ligament/tendon tissue engineering. J Nanobiotechnology **18**: 23. DOI: 10.1186/s12951-019-0556-1.

Subramanian G, Stasuk A, Elsaadany M, Yildirim-Ayan E (2017) Effect of uniaxial tensile cyclic loading regimes on matrix organization and tenogenic differentiation of adipose-derived stem cells encapsulated within 3D collagen scaffolds. Stem Cells Int **2017**: 6072406. DOI: 10.1155/2017/6072406.

Testa S, Costantini M, Fornetti E, Bernardini S, Trombetta M, Seliktar D, Cannata S, Rainer A, Gargioli C (2017) Combination of biochemical and mechanical cues for tendon tissue engineering. J Cell Mol Med **21**: 2711-2719.

Tsai PI, Chen CY, Huang SW, Yang KY, Lin TH, Chen SY, Sun JS (2018) Improvement of bone-tendon fixation by porous titanium interference screw: a rabbit animal model. J Orthop Res **36**: 2633-2640.

Tudor-Locke C, Aguiar EJ, Han H, Ducharme SW, Schuna JM, Jr., Barreira TV, Moore CC, Busa MA, Lim J, Sirard JR, Chipkin SR, Staudenmayer J (2019) Walking cadence (steps/min) and intensity in 21-40 year olds: CADENCE-adults. Int J Behav Nutr Phys Act **16**: 8. DOI: 10.1186/s12966-019-0769-6.

Tudor-Locke C, Craig CL, Brown WJ, Clemes SA, De Cocker K, Giles-Corti B, Hatano Y, Inoue S, Matsudo SM, Mutrie N, Oppert JM, Rowe DA, Schmidt MD, Schofield GM, Spence JC, Teixeira PJ, Tully MA, Blair SN (2011) How many steps/day are enough? For adults. Int J Behav Nutr Phys Act **8**: 79. DOI: 10.1186/1479-5868-8-79.

Tulloch SJ, Devitt BM, Norsworthy CJ, Mow C (2019a) Synovitis following anterior cruciate ligament reconstruction using the LARS device. Knee Surg Sports Traumatol Arthrosc **27**: 2592-2598.

Tulloch SJ, Devitt BM, Porter T, Hartwig T, Klemm H, Hookway S, Norsworthy CJ (2019b) Primary ACL reconstruction using the LARS device is associated with a high failure rate at minimum of 6-year follow-up. Knee Surg Sports Traumatol Arthrosc **27**: 3626-3632.

Wang JH (2006) Mechanobiology of tendon. J Biomech **39**: 1563-1582.

Wang S, Ge Y, Ai C, Jiang J, Cai J, Sheng D, Wan F, Liu X, Hao Y, Chen J, Chen S (2018a) Enhance the biocompatibility and osseointegration of

polyethylene terephthalate ligament by plasma spraying with hydroxyapatite *in vitro* and *in vivo*. Int J Nanomedicine **13**: 3609-3623.

Wang T, Chen P, Zheng M, Wang A, Lloyd D, Leys T, Zheng Q, Zheng MH (2018b) *In vitro* loading models for tendon mechanobiology. J Orthop Res **36**: 566-575.

Wang T, Thien C, Wang C, Ni M, Gao J, Wang A, Jiang Q, Tuan RS, Zheng Q, Zheng MH (2018c) 3D uniaxial mechanical stimulation induces tenogenic differentiation of tendon-derived stem cells through a PI3K/AKT signaling pathway. FASEB J **32**: 4804-4814.

Wang XM, Ji G, Wang XM, Kang HJ, Wang F (2018d) Biological and biomechanical evaluation of autologous tendon combined with ligament advanced reinforcement system artificial ligament in a rabbit model of anterior cruciate ligament reconstruction. Orthop Surg **10**: 144-151.

Wood TJ, Leighton J, Backstein DJ, Marsh JD, Howard JL, McCalden RW, MacDonald SJ, Lanting BA (2019) Synthetic graft compared with allograft reconstruction for extensor mechanism disruption in total knee arthroplasty: a multicenter cohort study. J Am Acad Orthop Surg **27**: 451-457.

Yeom BY, Pourdeyhimi B (2011) Web fabrication and characterization of unique winged shaped, area-enhanced fibers via a bicomponent spunbond process. J Mater Sci **46**: 3252-3257.

Yu SB, Yang RH, Zuo ZN, Dong QR (2014) Histological characteristics and ultrastructure of polyethylene terephthalate LARS ligament after the reconstruction of anterior cruciate ligament in rabbits. Int J Clin Exp Med **7**: 2511-2518.

Zhi Y, Jiang J, Zhang P, Chen S (2019) Silk enhances the ligamentization of the polyethylene terephthalate artificial ligament in a canine anterior cruciate ligament reconstruction model. Artif Organs **43**: E94-E108.

Zoltan DJ, Reinecke C, Indelicato PA (1988) Synthetic and allograft anterior cruciate ligament reconstruction. Clin Sports Med **7**: 773-784.

## Discussion with Reviewers

**Reviewer 1**: What is the novelty of the work? Previous works have already shown that different scaffolds coated with collagen and/or including CaP show improved cellular responses when compared to their uncoated controls.

**Authors**: The novelty of the present study was the development of a new type of PET artificial ligament with profiled cross-section filaments and biological modification. Since previous works have already shown that different scaffolds coated with collagen and/or including CaP show improved cellular responses than their uncoated controls, most of these researched or commercialised artificial ligaments are circular-shaped fibers. In addition to providing a higher surface-area-to-volume ratio than those with round cross-sections, the profiled cross-section fibers used in the present study had the characteristics of moisture-wicking fibres, which can help with the circulation of fluids through capillary action. Hence, they were more conducive to promoting cell growth. This new design is an effective strategy and can be considered an optional ligament augmentation device or synthetic graft for ligament reconstruction.

**Reviewer 2**: In addition to collagen coating, have you tried hyaluronic acid or chitosan coating on your PET/CaP filaments? If yes, what are the outcomes?

**Authors**: We have not yet used hyaluronic acid or chitosan coating on PET/CaP filaments. Previous studies by other groups have used hyaluronic acid or chitosan for artificial ligament modification, with pretty good results (Li *et al.*, 2013, additional reference). We will include it in our future research.

## Additional Reference

Li H, Jiang J, Ge Y, Xu J, Zhang P, Zhong W, Chen S (2013) Layer-by-layer hyaluronic acid-chitosan coating promoted new collagen ingrowth into a poly(ethylene terephthalate) artificial ligament in a rabbit medical collateral ligament (MCL) reconstruction model. J Biomater Sci Polym Ed **24**: 431-446.

**Editor's note**: The Scientific Editor responsible for this paper was Manuela Gomes.